Multiple production of particles and *s*-channel unitarity in the pomeron strong-coupling region

A. A. Migdal, A. M. Polyakov, and K. A. Ter-Martirosyan

(Submitted June 14, 1974)
Zh. Eksp. Teor. Fiz. **67**, 2009–2021 (December 1974)

A scale-invariant solution of the equations of the theory of interacting pomerons, corresponding to strong coupling of pomerons at ultra-high energies, is used to analyze processes of multi-pomeron production of particles and inclusive processes. It is shown that, because of the power-law decrease of the pomeron vertices in this solution, all the difficulties associated with the increase of the particle-production cross section as $\xi = \ln(s/\mu^2) \to \infty$ disappear and the *s*-channel unitarity requirements are restored.

The scale-invariant solution of the theory of interacting pomerons, obtained in previous articles[1,2]1) (cf. also[3]) by Wilson's ϵ-expansion method[4], corresponds to strong coupling at the theoretical ultra-high energies when $\xi = \ln(s/\mu^2) \gtrsim r^{-2}$ (where $r^{-2} \sim 100$). In this region the pomeron Green function G and the three-pomeron vertex Γ are found to differ appreciably from their "free" values $G_0 \sim \omega^{-1}$ and $\Gamma_0 \sim r$. The decrease of Γ as $\omega_1 \sim k_1^2 \sim \omega_2 \sim k_2^2 \to 0$ leads to the possibility of self-consistency of the system of equations of the Dyson-Schwinger type for G and Γ. These equations correspond exactly to the reggeon t-channel unitarity conditions[5].

It is extremely important to verify that the solution obtained does not contradict the s-channel unitarity conditions. For this we must construct, in the framework of this same solution, the amplitudes of the particle-production processes and, using these, verify at least the simplest consequences of s-channel unitarity. To this we devote the present article (cf. also[6]), in which multi-reggeon particle-production processes are considered and a theory of inclusive processes in the pomeron strong-coupling region, i.e., for ultra-high energies when $\xi = \ln(s/\mu^2) \to \infty$, is constructed.

1. MULTI-REGGEON PRODUCTION OF PARTICLES

We shall consider processes of production of $n' = n + 2$ particles in multi-reggeon kinematics[7,8] for $n \ll \xi$, when not only is $\xi \gg 1$, but also the difference $\xi_{i,i-1} = y_i - y_{i-1}$ in the rapidities of all neighbors in the scale of the fast particles (Fig. 1) is large: $\xi_{i,i-1} \gg \xi_0$. Here ξ_0 is a certain large number, such that for $\xi > \xi_0$ only pomeron exchange is important.

In these conditions the production amplitude $T_{2\to n+2}$ is determined[7] by the contribution of the multi-pomeron graphs of Fig. 2a. For free pomerons (i.e., for $r = 0$) this contribution is

$$\frac{1}{8\pi s} T^{(0)}_{2\to n+2} = g^2 \Gamma'^n \exp\left(-\sum_{i=1}^{n} k_i^2 \xi_{i,i-1}\right),$$

where $\Gamma' \approx \Gamma'_0$ is the vertex for emission of a particle by a pomeron.

We recall that for the total cross-sections

$$\sigma'_{n+2} = \int \frac{|T_{2\to n+2}|^2}{2s} d\tau_{n+2},$$

where

$$d\tau_{n+2} = (2\pi)^4 \delta^4(P_2 - P_1) \frac{d^3p_1}{2\varepsilon_1 (2\pi)^3} \cdots \frac{d^3p_{n+2}}{2\varepsilon_{n+2}(2\pi)^3}$$

is the statistical weight of the final state, this amplitude leads to values of the order of $\ln^n(\xi/n)\sigma^{el}$[8], which when summed increase by a power law as $s \to \infty$; for $\sigma^{tot} = \text{const}$ this leads to violation of s-channel unitarity.

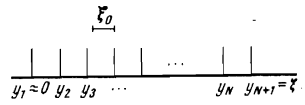

FIG. 1

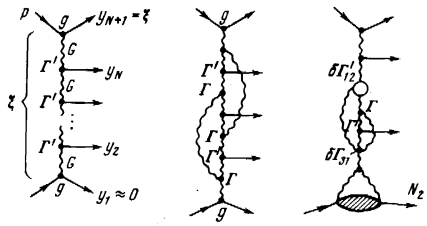

FIG. 2

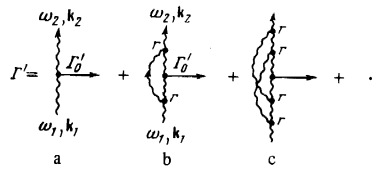

FIG. 3

Allowance for the interaction of the pomerons radically changes the whole picture. First, in the pole graph of Fig. 2a we must substitute the exact Green functions $G(\omega_i, k_i^2)$ of the pomerons and the exact vertices $\Gamma'(\omega_i, k_i; \omega_j, k_j)$ for emission of particles by pomerons. Secondly, in addition to this graph there appears the series of "enhanced" multi-pomeron graphs of Fig. 2b. Their contribution, by virtue of the scaling condition (3.10) in I, will be of the same order as the contribution of the pole graph of Fig. 2a (with the exact functions G and Γ). In addition, a small contribution will be made by the series of incompletely enhanced graphs of the type in Fig. 2c, containing vertices N_n, $\delta\Gamma_{nm}$ and $\delta\Gamma'_{nm}$, where $\delta\Gamma'_{nm}$ is the vertex for the emission of a particle in the transformation of n pomerons into m.

First we shall estimate the cross-sections $\tilde{\sigma}'_{N+2}$ taking into account only the contribution of the pole graphs of Fig. 2a with the exact G and Γ. It is clear that allowance for all the remaining graphs of Figs. 2b and 2c will not change the estimate obtained. For the estimate we need the vertex Γ' (Fig. 3) for the emission of a particle by a pomeron. Its general form in the strong-coupling region is analogous to that of Γ in (3.8) in I:

$$\Gamma'(\omega_1 k_1, \omega_2 k_2) = Z_0^{-1} R_0^{d/2} \omega^{\gamma'} F_1\left(\frac{R_0^2 k_1^2}{\omega_1^\nu}, \frac{R_0^2 k_2^2}{\omega_2^\nu}, \frac{R_0^2 k^2}{\omega^\nu}, \frac{\omega_2}{\omega_1}\right); \quad (1)$$

here Z_0 and R_0 are unknown constants, and the indices ν and

$$\gamma' = \varepsilon/6 + O(\varepsilon^2) \approx 1/3 \quad (2)$$

were determined in I; F_1 is an unknown universal function.

In place of the scaling condition (3.10) in I, the condition satisfied by the vertex Γ' in the strong-coupling region is

$$W = \Gamma'^2 G^2 \omega k^d \sim \omega^\beta,$$

in which, since $G \sim \omega^{-1-\eta}$, $\Gamma' \sim \omega^{\gamma'}$ and $k^2 \sim \omega^\nu$, we have

$$\beta = 2\gamma' + 1/2 \nu d - 1 - 2\eta = 1 - 1/4 \varepsilon + O(\varepsilon^2) \approx 1/2. \quad (3)$$

This condition is conveniently used to estimate the contribution of the graphs of Fig. 4, which (like the graph 7 in I for σ^{el}) determine the magnitudes σ'_{N+2} of the cross-sections of multi-pomeron processes.

The contribution of the graph in Fig. 4 is easily estimated in the ω,**k** representation. In analogy with the estimate of the graph of Fig. 7 in I for σ^{el}, we obtain

$$\sigma'_{N+2} \sim (G^2)^{N+1} \Gamma'^N (\omega k^d)^{N+1},$$

i.e.,

$$\sigma'_{N+2} \sim \sigma^{el}(\xi) W^N \sim \sigma^{el}(\xi)/\xi^{N\Delta},$$

where σ^{el} is the elastic-scattering cross section (4.9) in I. Since $\beta \approx 1/2 > 0$, as the number N of particles being formed increases the cross sections σ'_{N+2} decrease rapidly as $\xi \to \infty$. This is a consequence of the rapid decrease of the vertices Γ' as $\omega_i \to 0$, and fundamentally distinguishes the theory of interacting pomerons from the case of free pomerons with $\Gamma' = \gamma_0 = \text{const}$. When the cross sections σ'_{N+2} have the form (3) the s-channel unitarity condition $\sum_N \sigma'_{N+2} < \sigma^{tot}$ is always fulfilled for $\xi \to \infty$.

We note that, as has been shown in general form[9], the vertex Γ' for $\omega_1 \sim \omega_2 \sim 1/\xi$ should satisfy the inequality $|\Gamma'|^2 < |\Gamma| \cdot \text{const}$, i.e., in the power form of these vertices we should have

$$\gamma' \geqslant \gamma/2.$$

This condition is fulfilled in first order in ϵ, when $\gamma' = \gamma/2$, and is also fulfilled[10] to order ϵ^2 (in fact, however, the vertex Γ_1 determining the cross sections of the inclusive processes, and not the vertex Γ, should appear in the right-hand side in this condition. This vertex is considered in the next section and coincides with Γ in first order in ϵ).

We shall obtain an estimate for the cross sections σ'_{N+2}, taking into account the contribution to the multiperipheral amplitude $T_{2\to N+2}(\xi, \mathbf{k}; y_1, \mathbf{k}_1; y_2, \mathbf{k}_2; \ldots; y_N, \mathbf{k}_N)$

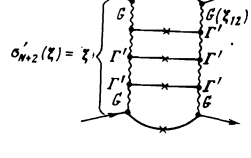

FIG. 4

from all the pomeron graphs. The general definition of the production amplitude is given by the formula

$$\frac{1}{8\pi s} T_{2\to N+2} = \int \exp[i(\mathbf{k}\rho + \mathbf{k}_1\rho_1 + \ldots + \mathbf{k}_N\rho_N)] \times a_{N+2}(\rho, \xi; \rho_1, y_1, \ldots, \rho_N, y_N) \frac{d^2\rho d^2\rho_1 \ldots d^2\rho_N}{(2\pi)^{N+1}}, \quad (4)$$

$$a_{N+2} = i\langle 0 | V(\rho, \xi) \Gamma'(\rho_1, y_1) \ldots \Gamma'(\rho_N, y_N) V^+(0,0) \times \exp\left[i \int (\mathscr{L} + \delta\mathscr{L}') \frac{d^2\rho'}{2\pi} d\xi' \right] |0\rangle. \quad (5)$$

As before, $y = 0, y_1, y_2, \ldots, y_N = \xi$ are the rapidities of the particles being produced (Fig. 1), and $\Gamma'(\rho, y)$ denotes the operator of the emission of a particle by pomerons:

$$\hat{\Gamma}'(\rho, y) = \gamma_0 \psi^+ \psi + \sum_{n+m>2} \delta\hat{\Gamma}_{nm}', \quad \delta\hat{\Gamma}_{nm}' = \gamma_{nm} \frac{i^{n-m}}{n!m!} (\psi^n \psi^{+m} + \psi^m \psi^{+n});$$
$$V(\rho, \xi) = g\psi(\rho, \xi) + \sum_n \delta V_n(\rho, \xi), \quad \delta V_n = \frac{N^{(n)}}{n!} \psi^n(\rho, \xi). \quad (6)$$

The quantity $\mathscr{L}$ is defined by formula (1.3) in I, and

$$\delta\mathscr{L}' = \sum_{n,m} \frac{\lambda_{nm}}{n!m!} i^{n-m} (\psi^n \psi^{+m} + \psi^m \psi^{+n}).$$

The first term $\gamma_0 \psi^+ \psi$ in Γ' corresponds to the emission of particles by a pomeron and corresponds to the vertices in the pole graphs of Fig. 2a. The remaining terms, proportional to γ_{nm}, give small contributions containing negative powers of ξ and correspond to the incompletely enhanced graphs of Fig. 2c, containing the vertices $\delta\Gamma'_{nm}$. One can verify that these formulas for $T_{2\to N+2}$ are correct by expanding the exponential in a series in powers of r and λ_{nm}, which reproduces exactly the contribution of all the pomeron graphs of Fig.2.

The total cross section $\sigma'_{N+2}(\xi)$ for multi-pomeron production of particles is

$$\sigma'_{N+2} = \int\limits_{\xi_i, \xi_{i+1} \geqslant \xi_0} C_N \left| \frac{T_{2\to N+2}}{8\pi s} \right|^2 \frac{d\mathbf{k} d\mathbf{k}_1 \ldots d\mathbf{k}_N}{(2\pi)^{(N+1)d/2}} dy_1 dy_2 \ldots dy_N = \int\limits_{\xi_i, \xi_{i+1} \geqslant \xi_0} C_N |a_{N+2}|^2 \frac{d\rho d\rho_1 \ldots d\rho_N}{(2\pi)^{(N+1)d/2}} dy_1 dy_2 \ldots dy_N, \quad (7)$$

where it is convenient, in the estimates by the ϵ-expansion method, to assume noninteger d: $d = 4 - \epsilon$ (although, of course, the estimates can also be performed for d = 2, and this will change them slightly).

The property of scale invariance, which holds in the strong-coupling region, means that the amplitudes (5) have the following structure:

$$a_{N+2} = \xi^{-2\Delta - N\delta} b_{N+2}(\rho/\xi^{\nu/2}, \rho_i/\xi^{\nu/2}, y_i/\xi), \quad (8)$$

where Δ and δ are the dimensions of the operators $\psi(\rho, \xi)$ and $\Gamma'(\rho, \xi)$, and b_{N+2} is a certain function of the variables indicated and is a quantity of order unity.

With this form of a_{N+2} formula (7) gives

$$\sigma'_{N+2} = I_N \xi^{-\alpha - N\beta}, \quad I_N = \int C_N |b_{N+2}(\mathbf{y}, \mathbf{y}_i, x_i)| \frac{d\mathbf{y} d\mathbf{y}_1 \ldots d\mathbf{y}_N}{(2\pi)^{(N+1)d/2}} dx_1 dx_2 \ldots dx_N, \quad (9)$$

where $\mathbf{y} = \rho/\xi^{\nu/2}$, $\mathbf{y}_i = \rho_i/\xi^{\nu/2}$, $x_i = y_i/\xi$ and where

i.e.,

$$-\alpha - N\beta = -4\Delta - 2N\delta + N + (N+1)\nu d/2,$$
$$\alpha = 4\Delta - \nu d/2 = \nu d/2 - 2\eta = 2 - 7\varepsilon/12 + O(\varepsilon^2) \approx 5/6,$$
$$\beta = 2\delta - 1 - \nu d/2.$$

In the expression for α we have substituted the quantity

$$\Delta = \nu d/4 - \eta/2 = 1 - \varepsilon/2 + O(\varepsilon^2) \approx 1/2.$$

which was already known to us (cf. I, (3.15)).

In order to obtain the ϵ-expansion of the power δ, we shall obtain an estimate of the amplitude a_{N+2} for the simplest case N = 1, writing it in the form[2)] $\sim G\Gamma'G$, and compare the estimate obtained with (8). This enables us to find δ in the form

$$\delta = \nu d/2 - \eta + \gamma/2 = 2 - \varepsilon/3 + O(\varepsilon^2) \approx 4/3 \qquad (10)$$

and, naturally, will give exactly the value (3) for β.

The formula (9) gives an estimate of the amplitude (5) in the limit as $\xi \to \infty$, corresponding to the neglect of the term $\delta\mathscr{L}'$ in (5), the terms δV_n in the operator V, and the terms proportional to γ_{nm} in (6). Allowance for all these terms leads to the incompletely enhanced graphs of Fig. 2c, containing the vertices $\delta\Gamma_{nm}$, $N^{(n)}$ and $\delta\Gamma'_{nm}$ respectively. Compared with all the enhanced graphs (Figs. 2a and 2b), the contribution of these graphs in the first two cases contains small factors, as in the case of the elastic-scattering amplitude. An estimate of the vertex $\delta\Gamma'_{nm}$ can be carried out by the ϵ-expansion method, which gives for it a value of the same order of magnitude as $\delta\Gamma_{nm}$. Therefore, the relative smallness of the graphs containing the vertices $\delta\Gamma'_{nm}$ is exactly the same as that of the graphs with the vertex $\delta\Gamma_{nm}$.

The arguments adduced show that the contributions of the incompletely enhanced graphs for $\xi \to \infty$ are small and enable us to obtain an estimate of them immediately from the form of the graph (or from the type of the term $\delta\hat{\mathscr{L}}, \delta\hat{V}$ and $\delta\Gamma'$) taken into consideration in (5).

2. INCLUSIVE PROCESSES IN THE STRONG-COUPLING REGION

The particle production processes are characterized by the inclusive cross-section

$$\frac{d\sigma_{incl}}{dy d\mathbf{p}_\perp} = \sum_N \sum_{i=1}^N \int d\sigma_N(y_i, \mathbf{p}_{i\perp}) \delta(y - y_i) \delta(\rho_\perp - \rho_{i\perp}) \qquad (11)$$

for the emergence of one of the particles produced into a given phase-space element $d\tau(\mathbf{p}) = d^3\mathbf{p}/E = dy d\mathbf{p}_\perp$; here $y = \ln(p_z/\mu)$ is the rapidity and $d\sigma_N(y_i, \mathbf{p}_{i\perp})$ is the differential cross section for production of N particles with given momenta $\mathbf{p}_i = (y_i, \mathbf{p}_{i\perp})$.

We shall call the quantity

$$\rho(\xi, y) = \frac{1}{\sigma^{tot}(\xi)} \int \frac{d\sigma_{incl}}{dy d\mathbf{p}_\perp} d\mathbf{p}_\perp, \qquad (12)$$

the inclusive spectrum in the rapidity space; its integral over the energy dE = Edy is the total incoming energy E_0:

$$\int_0^\xi E\rho dy = \frac{1}{\sigma^{tot}} \sum_N \int \sum_{i=1}^N E_i d\sigma_N = E_0 \frac{1}{\sigma^{tot}} \sum_N d\sigma_N = E_0, \qquad (13)$$

and its integral over the rapidity is the mean multiplicity:

$$\int_0^\xi \rho(\xi, y) dy = \sum_N N \frac{\sigma_N}{\sigma^{tot}} = \bar{N}(\xi). \qquad (14)$$

1) Middle part of the spectrum: $y \sim \xi/2$. In the multiperipheral Regge-pole model the inclusive cross section for $y \sim \xi/2$, $\xi \to \infty$ is determined by the contribution of the two-pomeron graph of Fig. 5a, in the form

$$\frac{1}{\sigma_0^{tot}} \frac{d\sigma^0_{incl}}{dy d\mathbf{p}_\perp} = f(p_\perp^2)\theta(y)\theta(\xi - y), \qquad (15)$$

i.e.,

$$\rho(\xi, y) = \rho_0 \theta(y)\theta(\xi - y) = \text{const}, \quad 0 \leq y \leq \xi,$$

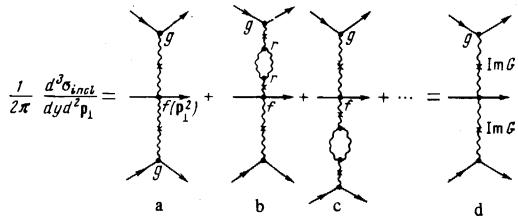

FIG. 5

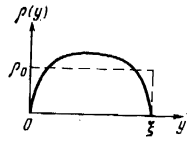

FIG. 6. The function $\rho(y)$; $\rho \sim [y(\xi - y)]^{1/6}$ – solid curve; $\rho \sim$ const – dashed curve.

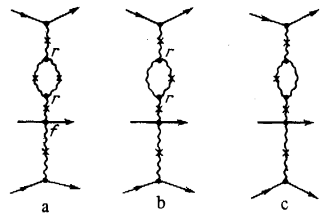

FIG. 7

where $\rho_0 = f(p_\perp^2) dp_\perp$. Correspondingly, the total multiplicity increases logarithmically with the energy:

$$\bar{N}(\xi) = \rho_0 \xi. \qquad (16)$$

This plane (Feynman or multiperipheral) spectrum $\rho = \rho_0$ in rapidity space is indicated by the dashed line in Fig. 6. We shall find all these quantities in our theory in the strong-coupling region, i.e., for $r^2\xi \gtrsim 1$.

The first corrections in perturbation theory in the three-pomeron interaction are determined by the graphs in Figs. 5b and 5c. In these graphs, as in the principal graph of Fig. 5a, lines of "cut" reggeons are denoted by a cross. Their contribution is

$$\mathrm{Im}[\eta_+(\alpha_P) G(\xi, k^2)] = G(\xi, k^2),$$

where $\eta_+(\alpha_P)$ is the signature factor. The vertices for these lines are the same as for the ordinary pomeron lines; therefore, the contribution of the graphs in Fig. 5 is determined by the same rules[11] as in the case of the elastic-scattering amplitude. These rules have been elucidated in detail by Abramovsky, Gribov and Kancheli[11]. They noted a number of subtleties, but these are not important for us just now. For example, in[11] the vertices in Fig. 5b correspond not to ir but to r, and therefore the contribution ρ_a of the graph in Fig. 5b is opposite in sign to that in the case of Fig. 2 in I. However, besides the graph in Fig. 5b there are also the three graphs of Fig. 7, in which the contribution of the graph in Fig. 7a is $2\rho_a$, and the contribution of each of the graphs in Figs. 7b and 7c is $-2\rho_a$. Therefore, in total, the contribution of all these graphs is $-\rho_a$. For simplicity, by a convention we shall speak below of only the one graph Fig. 5b, meaning, in fact, the resultant contribution of all these graphs. An analogous situation also obtains in the case of more complicated graphs. The calculation must be performed in the ξ,k representation, where the integration is performed over the coordinates $\xi_1, \xi_2, \ldots$ of the three-pomeron vertices. The coordinate y of the vertex $f(p_\perp^2)$ is held fixed.

For the following it is important that graphs of the form of Fig. 8 with pomeron lines bypassing the vertex

$f(p_\perp^2)$ make no contribution since in each order their contributions cancel each other. This was noted by Abramovsky, Gribov and Kancheli[11], and greatly simplifies all the calculations.

The total contribution of all the graphs of Fig. 5 is expressed in terms of the exact pomeron Green functions $G(y,k^2)$ for $k^2 = 0$, in a form corresponding to the one graph d on the right in Fig. 5:

$$\frac{d\sigma_{incl}}{8\pi dy d\mathbf{p}_\perp} = \frac{g_0^2}{\pi} f(p_\perp^2) G(y,0) G(\xi - y, 0), \tag{17}$$

or, which is equivalent, in terms of the total cross sections, in the form

$$\frac{d\sigma_{incl}}{dy\, d\mathbf{p}_\perp} = \frac{f(p_\perp^2)}{8\pi^2 g_0^2} \sigma^{tot}(y) \sigma^{tot}(\xi - y), \tag{18}$$

i.e.,

$$\rho(\xi, y) = \frac{\rho_0}{8\pi g_0^2} \frac{\sigma^{tot}(y)\sigma^{tot}(\xi - y)}{\sigma^{tot}(\xi)}.$$

In the strong-coupling region, where these formulas are valid, we have

$$\sigma^{tot}(y) = \frac{8\pi g^2}{\Gamma(1+\eta)} y^\eta.$$

Therefore, the inclusive spectrum (18) is nonuniform:

$$\rho(\xi, y) = \frac{Z_0 \rho_0}{\Gamma(1+\eta)} \left(\frac{y(\xi - y)}{\xi}\right)^\eta. \tag{19}$$

The total multiplicity in our theory increases with energy more rapidly than in the multiperipheral model (i.e., than in (16)):

$$\bar{N}(\xi) = \int \rho(\xi, y)\, dy = \frac{Z_0 \rho_0 \Gamma(1+\eta)}{\Gamma(2+2\eta)} \xi^{1+\eta}. \tag{20}$$

The graph of the function (19) for $\eta \simeq 1/6$ is shown in Fig. 6.

In the spectrum (19) most of the particles are in the region of "pionization," with $y \approx \xi/2$, and the density decreases near the edges of the spectrum. This result can be understood by analogy with the density of a gas in the one-dimensional rapidity space $0 \le y \le \xi$.

The Feynman spectrum $\rho = \rho_0 = \text{const}$ (15) corresponds to the gas density that is established for short-range forces. The reggeon interaction (of the type in Figs. 5b, 5c, etc.) of the particles corresponds to long-range in rapidity space, leading to long-range correlations that do not fall off but increase with increasing distance Δy. In such a system the conditions necessary for the appearance of a statistical limit of the distribution in y as $\xi \to \infty$ are not fulfilled. Therefore, even as $\xi \to \infty$, the density $\rho(y)$ of the gas depends on the distance from the boundaries y = 0 and $y = \xi$. (It increases toward the middle of the interval because of the effective repulsion between the particles and the boundaries.)

2) Rigid boundary of the spectrum. In the region of the rigid part of the spectrum, for $m/E_0 < 1 - x \ll 1$, where $x = p_z/E_0$, the inclusive cross section is determined by the process of diffraction production of a heavy shower with mass $M^2 \approx (1-x)s \gg \mu^2$. In the case of free pomerons it corresponds to the contribution of the simplest (three-pomeron) graph Fig. 9a and is determined by the Kancheli-Mueller formula[12]

$$\frac{d\sigma_{incl}}{8\pi d\xi d\mathbf{p}_\perp} = \frac{g_0^3 r \sqrt{\alpha_0'}}{2\pi} (1-x)^{2(1-\alpha_p(-p_\perp^2))} = \frac{g_0^3 r \sqrt{\alpha_0'}}{2\pi} \exp(-2\alpha_0' p_\perp^2 \eta), \tag{21}$$

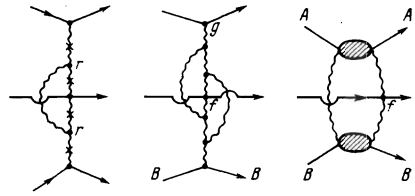

FIG. 8

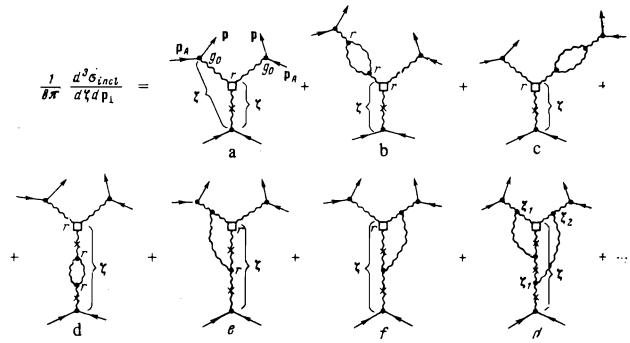

FIG. 9

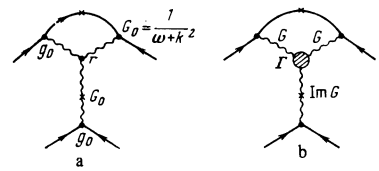

FIG. 10

where, for $\zeta = \xi - \eta = \ln(M^2/\mu^2)$ ($\eta = \ln(s/M^2) = \ln[1/(1-x)]$), we have used for the pomeron-nucleon interaction cross-section (11) $\sigma_{PN}(M^2, k^2)$ its pomeron asymptotic from $\sigma_{PN} \approx 8\pi g_0 r$. The normalization in (21) is determined by the condition that

$$\frac{\sigma_{incl}}{8\pi} = \int \frac{d\sigma_{incl}}{8\pi d\zeta d\mathbf{p}_\perp} d\zeta d\mathbf{p}_\perp$$

be the contribution of the graph Fig. 10a.

We recall that formula (21) leads[8] to contradiction with the relation

$$\int_0^1 x\rho(\xi, \zeta) \frac{dx}{x} = 1.$$

Indeed, since $d\zeta = d\eta = dx/(1-x)$, this relation leads to the inequality

$$\sigma'_{incl} = \int_{\zeta_0}^{\xi - \zeta_1} d\zeta \int \frac{d\sigma_{incl}}{d\zeta d p_\perp} dp_\perp \le \sigma^{tot}, \tag{22}$$

where $\zeta_0, \zeta_1 < \xi$ are any positive numbers. On substituting (21) into the left-hand side we obtain a quantity increasing like $\ln\xi$ as $\xi \to \infty$. Therefore, for $r \neq 0$ and for $\sigma^{tot} = \text{const}$, the inequality (22) is always violated in the limit $\xi \to \infty$.

We shall show that allowance for the pomeron interactions removes this contradiction as a consequence of the screening, and effective decrease, of the vertex r.

In the general case the cross-section $d\sigma_{incl}/d\zeta dp_\perp$ is determined by the contribution of all graphs of the form of Fig. 9. The integration in them (in the ξ,k representation) is taken over the rapidities of all the vertices apart from the one denoted by a square in Fig. 9; the rapidity corresponding to this vertex remains constant, equal to $\zeta = \ln(M^2/\mu^2)$. The contribution of the

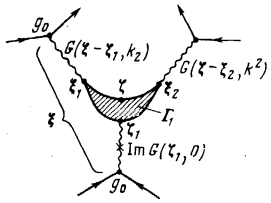

FIG. 11

graphs is calculated by the same rules as in the case of Fig. 5. Denoting by

$$\rho'(\xi,\ \zeta,\ p_\perp^2)=d\sigma_{incl}/8\pi d\zeta d^2p_\perp \qquad (23)$$

the total contribution of the graphs in Fig. 9, we obtain, integrating (23) over ζ and $p_\perp$, the magnitude of the contribution (22) of the rigid part of the inclusive spectrum to the total cross section:

$$\frac{1}{8\pi}\sigma_{incl}=\int_0^\xi d\zeta\int\rho(\xi,\zeta,p_\perp^2)d^2p_\perp=\varphi(\xi).$$

This quantity is the contribution of the graph of Fig. 10b, which differs from the graph of Fig. 10a in that it contains the exact pomeron vertex Γ and exact propagators $G(\omega,k^2)$. In the ω representation the contribution of this graph is

$$\varphi(\omega)=\int_0^\infty e^{-\omega\xi}\varphi(\xi)d\xi=g_0\Sigma_1(\omega,0)G(\omega,0), \qquad (24)$$

where

$$\Sigma_1(\omega,0)=g_0^2\int\Gamma(\omega',\mathbf{k},\omega-\omega',\mathbf{k})G(\omega',k^2)G(\omega-\omega',k^2)\frac{d^2k}{2\pi\alpha_0'}$$

is a quantity which differs by only a factor from the pomeron self-energy $\Sigma(\omega,0)$. As we have seen above, in the strong-coupling region,

$$\Sigma_1(\omega,\ 0)=\Sigma_1(0,\ 0)+a\omega+b\omega^{1+\eta},$$

where a and e are certain constants. In the region of small ω only the first term is important here, and therefore $\varphi(\xi)\propto\xi^\eta$, i.e., σ_{incl} increases no more rapidly than the total cross-section as $\xi\to\infty$. Since $\sigma'_{\text{incl}}<\sigma_{\text{incl}}=8\pi\varphi(\xi)$, the left-hand side of (24) also increases no faster than the total cross section as $\xi\to\infty$, and this removes the contradiction with the inequality (22), i.e., with the requirement of s-channel unitarity, as $\xi\to\infty$.

We shall obtain a general expression for the inclusive cross section $\rho'(\xi,\zeta,p_\perp^2)$ and calculate it in the form of the ϵ-expansion. The total contribution of the graphs of Fig. 9 has a structure corresponding to the graph of Fig. 11:

$$\rho'=\frac{g_0^3}{2\pi}\int_\zeta^\xi d\xi_1\int_\zeta^\xi d\xi_2\int_0^\zeta d\zeta_1 G(\xi-\xi_1,k^2)G(\xi-\xi_2,k^2)\Gamma_1G(\xi_1,0), \qquad (25)$$

where

$$\Gamma_1\equiv\Gamma_1(\xi_1-\zeta_1,\ \mathbf{k};\ \xi_2-\zeta_2,\ \mathbf{k}',\ \zeta-\zeta_1)$$

is the four-point vertex–the contribution of the graphs of the form Fig. 12. It appears in (25) for $\mathbf{k}'=\mathbf{k}$ and differs from the three-reggeon vertex $\Gamma(\xi_1-\zeta_1,\mathbf{k};\ \xi_2-\zeta_2,\mathbf{k}')$, which in the ξ representation is an integral of Γ_1, of the form

$$\Gamma=\int_{\zeta_1}^{\min(\xi_1,\xi_2)}\Gamma_1d\zeta_1.$$

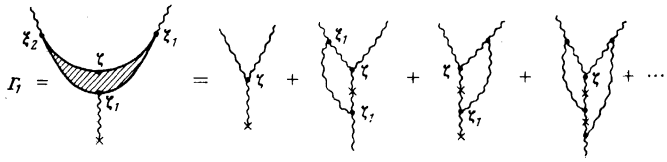

FIG. 12

In this representation, the estimate of Γ in accordance with formula (3.5) in I is

$$\Gamma\sim Z_0^{-3/2}R_0^{d/2}\xi^{-2-\gamma},\qquad \xi=\min(\xi_1-\zeta_1,\ \xi_2-\zeta_2).$$

Therefore,

$$\Gamma_1\sim Z_0^{-3/2}R_0^{d/2}\xi^{-3-\gamma}.$$

In the pomeron strong-coupling region the function ρ' has, like G and Γ, a scale-invariant form:

$$\rho'=C\xi^\lambda\chi(k^2R_0^2\xi^\nu,\ z), \qquad (26)$$

where $z=\zeta/\xi$; λ and χ are a universal number and function, and $C=(g_0^3/2\pi)Z_0^{3/2}R_0^{d/2}$ is a constant depending on r. Since $G(\xi,k^2)\sim\xi^\eta$, and $\Gamma_1\sim\xi^{-3-\gamma}$, we have

$$\lambda=3\eta-\gamma=-\varepsilon/12+O(\varepsilon^2)\approx-1/6. \qquad (27)$$

We shall find the explicit form of the function $\chi(y,z)$ by writing ρ' in (26) in the form of its ϵ-expansion

$$\rho'=\frac{g_0^3}{2\pi}Z_0^{3/2}R_0^{d/2}e^{\lambda\ln\xi}\chi_0(1+\varepsilon\chi_1+\ldots), \qquad (28)$$

where $\chi_i=\chi_i(y,z)$, and comparing it, for $r^2=2\epsilon/3$, with the expansion of ρ' in perturbation-theory series in 4-dimensional space.

For simplicity, we shall carry out the calculations for $p_\perp^2=\alpha_0'k^2=0$. To terms of order r^3, the six graphs of Figs. 9a–f make a contribution to ρ'. The first four of these (a–d), which determine the contribution of order r and the correction to it from $\Sigma(\omega,k^2)$, give in the $\xi,\mathbf{k}$ representation

$$\rho_1'=\frac{g_0^3r}{2\pi}\left\{1+\frac{r^2}{8}(2\ln(\xi-\zeta)+\ln\zeta+\text{const})\right\}.$$

The next two graphs (e,f) of Fig. 9 give equal contributions and are easily calculated in the $\xi,\mathbf{k}$ representation:

$$\Delta\rho'=-\frac{g_0^3r}{4\pi}\left\{\ln\zeta-\ln\frac{\xi}{\xi-\zeta}+\text{const}\right\}.$$

In total, we obtain

$$\rho'=\frac{g_0^3r}{2\pi}\left\{1+\frac{r^2}{4}\left(\frac{3}{2}\ln\frac{1}{z}+\ln\frac{1}{1-z}\right)-\frac{r^2}{8}\ln\xi+\text{const}\right\},$$

where $z=\zeta/\xi$. Comparison with (28) for $r^2=2\epsilon/3$ gives

$$\chi=\chi_0(1+\varepsilon\chi_1)=\left(\frac{2\varepsilon}{3}\right)^{1/2}\left\{1+\frac{\varepsilon}{6}\left(\frac{3}{2}\ln\frac{1}{z}+\ln\frac{2}{1-z}+\text{const}\right)\right\}. \qquad (29)$$

It has been taken into account that, to terms of order ϵ^2,

$$r^2\approx\frac{2\varepsilon}{3}(1+C\varepsilon),$$

i.e., $r=(2\epsilon/3)^{1/2}(1+C\epsilon/6)$, where C is a constant of order unity[10], unimportant for the following. It has also been taken into account that, according to formulas (3.12) and (3.17) from I,

$$Z_0^{3/2}R_0^2=(Z_0^{1/2}R_0)^3\frac{1}{R_0}\approx r\left(\frac{3}{2\varepsilon}\right)^{1/2}\left(1-\frac{\varepsilon}{24}\ln2\right),$$

since (cf. I) $R_0^{-1}\approx1-(1/24)\epsilon\ln2$ for $r^2\approx2/3\epsilon$.

From (28) and (29) follows the value (27) already obtained earlier for λ:

$$\lambda = -1/6 r^2 + O(r^4).$$

The value of χ given by (29) is correct only if $z = \zeta/\xi$ is not too small. For $\xi \to \infty$ and for small beam mass $\zeta \ll \xi$ the inclusive cross section (23) should behave like the diffraction production cross section

$$\frac{d\sigma_{diff}}{dp_\perp^2} \sim \frac{d\sigma_{el}}{dp_\perp^2} \sim \xi^{2\eta} \sim \xi^{\varepsilon/6}.$$

Formula (29) is compatible with this condition if we write it in the form

$$\chi = \left(\frac{2\varepsilon}{3}\right)^{1/2} z^{-\varepsilon/4}\left(1 + \frac{\varepsilon}{6}\ln\frac{1}{1-z} + \text{const}\cdot\varepsilon\right).$$

Discarding here the last factor, which is close to unity, we write the inclusive cross section (23), (28) in a form analogous to the case (21) of free pomerons:

$$\frac{d\sigma_{incl}}{2\pi d\zeta dp_\perp^2} = \frac{g^3}{2\pi} R_0 \xi^{-\varepsilon/12}\left(\frac{2\varepsilon}{3}\right)^{1/2}\left(\frac{\xi}{\zeta}\right)^{\varepsilon/4} = \left(\frac{\sigma^{tot}(\xi)}{8\pi}\right)^{3/2}\frac{\Gamma_{eff}}{2\pi}, \quad (30)$$

where

$$\Gamma_{eff} = (\alpha_0')^{1/2}\left(\frac{2\varepsilon}{3}\right)^{1/2}\frac{\xi^{\varepsilon/24}}{\zeta^{\varepsilon/4}}, \quad (\alpha_0')^{1/2} = R_0, \quad (31)$$

is the effective magnitude of the three-pomeron vertex (which replaces the constant r in (21)), and $(\delta^{tot}(\xi)/8\pi)^{3/2} = g^3\xi\epsilon/8$.

As can be seen, in the pomeron strong-coupling region the effective magnitude of the three-pomeron vertex is not small–for $\zeta \sim 1$ and $\xi \gg 1$ the ratio $\Gamma_{eff}/(\alpha_0')^{1/2}$ should be of order unity, and close to $(2\epsilon/3)^{1/2} = 2/\sqrt{3}$. The corresponding value of the inclusive cross section (30) is found to be 10 to 12 times greater than that observed in the experiment of [13] for the reaction $pp \to pX$ at the energies $E \sim 2 \times 10^3$ GeV attainable in the NAL and the ISR. This means that at these energies we are still not in the strong-coupling region, i.e., that the constant r is small: $r = \Gamma_{eff}(\alpha_0')^{-1/2}/10 \sim 1/10$. For such a small value of r the inclusive cross-section is determined not by (30) but by the first term of the expansion of ρ' in a perturbation-theory series, i.e., by formula (21).

[1)] Below, for brevity, we shall designate the paper [2] by I.

[2)] I.e., in the form of the pole value

$$a_3 = ig^2\int_{\hat{}}\frac{d\omega\, d\omega_1}{(2\pi i)^2}\exp(\omega\xi + \omega_1\xi_1) \times \int\frac{d\mathbf{k}\, d\mathbf{k}_1}{(N_d)^2}\exp[i(\mathbf{k}\rho + \mathbf{k}_1\rho_1)]\,G(\omega, k^2)\,\Gamma(\omega\mathbf{k}, \omega_1\mathbf{k}_1)\,G(\omega_1, k_1^2).$$

[1] A. A. Migdal, A. M. Polyakov and K. A. Ter-Martirosyan, Phys. Lett. **48B**, 239 (1974).

[2] A. A. Migdal, A. M. Polyakov and K. A. Ter-Martirosyan, Zh. Eksp. Teor. Fiz. **67**, 848 (1974) [Sov. Phys-JETP **40**, 420 (1975)].

[3] H. D. I. Abarbanel and J. B. Bronzan, Phys. Lett. **48B**, 345 (1974).

[4] V. N. Gribov and A. A. Migdal, Zh. Eksp. Teor. Fiz. **55**, 1498 (1968) [Sov. Phys.-JETP **28**, 784 (1969)].

[5] V. N. Gribov, I. Ya. Pomeranchuk and K. A. Ter-Martirosyan, Yad. Fiz. **2**, 361 (1965) [Sov. J. Nucl. Phys. **2**, 258 (1966)].

[6] V. N. Gribov, I. Ya. Pomeranchuk and K. A. Ter-Martirosyan, ITP Preprint, Chernogolovka, 1973; ITEP Preprint No. 102, 1973.

[7] K. A. Ter-Martirosyan, Zh. Eksp. Teor. Fiz. **44**, 341 (1963) [Sov. Phys.-JETP 17, 233 (1963)].

[8] I. A. Verdiev, O. V. Kancheli, S. G. Matinyan, A. M. Popova and K. A. Ter-Martirosyan, Zh. Eksp. Teor. Fiz. **46**, 1700 (1964) [Sov. Phys.-JETP 19, 1148 (1964)]; J. Finkelstein and K. Kajantie, Phys. Lett. **26B**, 305 (1968); Nuovo Cimento **56A**, 659 (1963).

[9] H. D. I. Abarbanel, V. N. Gribov and O. V. Kancheli, NAL-THY Preprint, 1972.

[10] M. Baker, Nucl. Phys. **B72** (1974).

[11] V. A. Abramovsky, V. N. Gribov and O. V. Kancheli, Proc. XVI Int. Conf. on High Energy Physics (Batavia, USA) 1, 1973 (p. 389).

[12] A. B. Kaĭdalov, Yu. F. Pirogov, N. L. Ter-Isaakyan and V. A. Khoze, ZhETF Pis. Red. **17**, 626 (1973) [JETP Lett. **17**, 440 (1973)]; L. I. Ya. F. (Leningrad Nuclear Physics Institute) Preprint No. 44, 1973.

[13] M. G. Albrow et al., Reports submitted to the XVI Int. Conf. on High Energy Physics, Batavia, USA, 1972; M. G. Albrow, A. G. Bagchus, D. P. Barber, et al., Nucl. Phys. **B51**, 388 (1973); **B54**, 6 (1973); M. Derrick, Report submitted to the Int. Seminar on Deep Inelastic Processes at High Energies, Dubna, 1973.

Translated by P. J. Shepherd.
215